

Method for characterization of Si waveguide propagation loss

Michele Moresco^{1,2}, Marco Romagnoli^{1,2,6,*}, Stefano Boscolo³, Michele Midrio³, Matteo Cherchi², Ehsan Shah Hosseini², Douglas Coolbaugh⁴, Michael R. Watts², and Birendra Dutt⁵

¹ PhotonIC Corporation, 5800 Uplander Way, Los Angeles, CA 90230, USA

² Massachusetts Institute of Technology, 77 Massachusetts Ave, Cambridge, MA 02139, USA

³ Dipartimento di Ingegneria Elettrica, Gestionale e Meccanica, Universita' di Udine, Udine 33100, Italy

⁴ College of Nanoscale Science and Engineering, University at Albany-State University of New York, 257 Fuller Rd., Albany, NY 12203, USA

⁵ Apic Corporation, 5800 Uplander Way, Los Angeles, CA 90230, USA

⁶ Marco Romagnoli's present address: CNIT (National Interuniversity Consortium for Telecommunications), via Moruzzi 1, 56124 Pisa, Italy

*marco.romagnoli@cnit.it

Abstract: A new method for measuring waveguide propagation loss in silicon nanowires is presented. This method, based on the interplay between traveling ring modes and standing wave modes due to back-scattering from edge roughness, is accurate and can be used for on wafer measurement of test structures. Examples of loss measurements and fitting are reported.

© 2013 Optical Society of America

OCIS codes: (230.5750) Resonators; (130.0130) Integrated optics; (230.7370) Waveguides; (230.3120) Integrated optics devices.

References and links

1. D. A. B. Miller, "Optical interconnects to electronic chips," *Appl. Opt.* **49**(25), F59–F70 (2010).
2. S. J. B. Yoo, "Future prospects of silicon photonics in next generation communication and computing systems," *Electron. Lett.* **45**(12), 584–588 (2009).
3. D. B. Keck and R. Tynes, "Spectral response of low-loss optical waveguides," *Appl. Opt.* **11**(7), 1502–1506 (1972).
4. S. Taebi, M. Khorasaninejad, and S. S. Saini, "Modified Fabry-Perot interferometric method for waveguide loss measurement," *Appl. Opt.* **47**(35), 6625–6630 (2008).
5. P. Dumon, W. Bogaerts, V. Wiaux, J. Wouters, S. Beckx, J. Van Campenhout, D. Taillaert, B. Luyssaert, P. Bienstman, D. Van Thourhout, and R. Baets, "Low-Loss SOI Photonic wires and ring resonators fabricated With deep UV lithography," *IEEE Photon. Technol. Lett.* **16**(5), 1328–1330 (2004).
6. J. Hu, V. Tarasov, A. Agarwal, L. Kimerling, N. Carlie, L. Petit, and K. Richardson, "Fabrication and testing of planar chalcogenide waveguide integrated microfluidic sensor," *Opt. Express* **15**(5), 2307–2314 (2007).
7. T. R. Bourk, M. M. Z. Kharadly, and J. E. Lewis, "Measurement of waveguide attenuation by resonance methods," *Electron. Lett.* **4**(13), 267–268 (1968).
8. K. K. Lee, D. R. Lim, L. Hsin-Chiao, and Agarwal, A. J. Foresi, L. C. Kimerling., "Effect of size and roughness on light transmission in a Si/SiO₂ waveguide: Experiments and model," *Appl. Phys. Lett.* **77**, 1617–1619 (2000).
9. M. Williamson and A. Neureuther, "Enhanced, quantitative analysis of resist image contrast upon line edge roughness (LER)," *Proc. SPIE* **5039**, 423–432 (2003).
10. T. Barwicz and H. A. Haus, "Three-dimensional analysis of scattering losses due to sidewall roughness in microphotonic waveguides," *J. Lightwave Technol.* **23**(9), 2719–2732 (2005).
11. K. K. Lee, D. R. Lim, L. C. Kimerling, J. Shin, and F. Cerrina, "Fabrication of ultralow-loss Si/SiO₂ waveguides by roughness reduction," *Opt. Lett.* **26**(23), 1888–1890 (2001).
12. B. E. Little, J. P. Laine, and S. T. Chu, "Surface-roughness-induced contradirectional coupling in ring and disk resonators," *Opt. Lett.* **22**(1), 4–6 (1997).
13. R. E. Collin, *Foundation for Microwave Engineering*, 2nd ed. (McGraw-Hill, N.Y., 2000).
14. A. Yariv, "Universal relations for coupling of optical power between microresonators and dielectric waveguides," *Electron. Lett.* **36**(4), 321–322 (2000).
15. Z. Zhang, M. Dainese, L. Wosinski, and M. Qiu, "Resonance-splitting and enhanced notch depth in SOI ring resonators with mutual mode coupling," *Opt. Express* **16**(7), 4621–4630 (2008).

1. Introduction

Silicon Photonics is becoming a technology for large bandwidth interconnection [1]. Moving from optical telecommunication to medium and short distance links requires a choice of technology that is more suitable for large volumes and low cost. Silicon Photonics is a good candidate because it exploits the established CMOS fabrication technology that is already widely developed for microelectronics [2]. In addition the compatibility of the processes facilitates the integration of photonics and electronics on the same chip. However, in order to implement large-scale production, with, for example 300mm wafers, in process control of the fabrication will be required. Testing is a part of the fabrication process that requires attention because can overcome the wafer cost itself.

The silicon waveguide is the basic building block of a silicon photonic circuit and the quality of the waveguide is also an indication of the quality of all the passive components of the circuit. In this paper we analyze a reliable method for the characterization of the waveguide loss that can implemented in specific test structures placed in any mask design for photonic wafers fabrication.

To the authors knowledge there is not a standard for waveguide loss measurement. Commonly used methods are cut back [3], Fabry-Perot loss modulation [4,5], variable length clips [6], and critical coupling configuration with all-pass single microring structures [7]. In this paper we propose a method based on a simple microring structure in and under coupled condition. This method has the advantage of being independent of input coupling losses or reflections and of being tolerant to the choice of the bus to ring gap size.

Commonly used Si nanowire waveguides have a cross-section of $220 \times 480 \text{ nm}$ and most of the propagation loss can be attributed to the side wall roughness [8]. Roughness is a typical result of the lithography and etch processes [9]. Typical values for the roughness are of the order of 2 nm with a correlation length of $\sim 40 \text{ nm}$. These values lead to a propagation loss of the order of 2 dB/cm [10]. Improved waveguide fabrication process will decrease the loss and as a consequence measurement becomes more challenging [11].

2. Theory

In this paper we propose a bus waveguide coupled to a microring structure, as shown in Fig. 1. The bus waveguide is $220 \times 400 \text{ nm}$ whereas the waveguide in the ring is $220 \times 480 \text{ nm}$. The width of the bus is shrunk to 400 nm in order to expand the mode further into the gap thus making its coupling to the microring more efficient. In the experiment the behavior for different bus to ring gaps ranging from 100 nm to 590 nm with incremental steps of 10 nm will be presented.

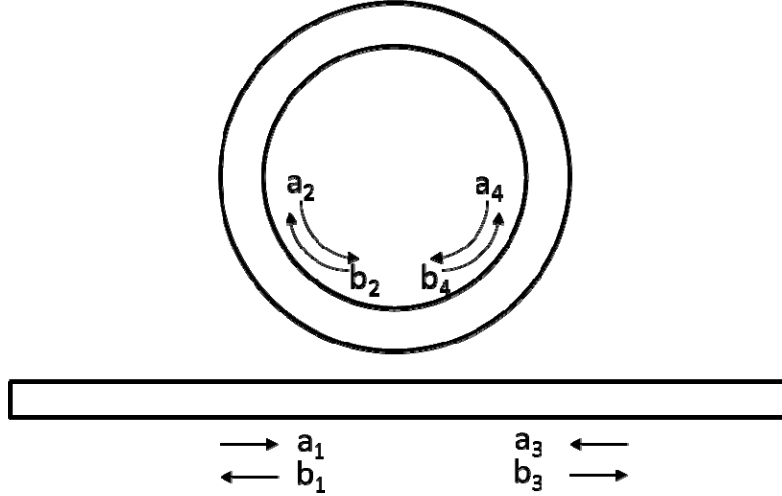


Fig. 1. Scheme of the bus waveguide coupled to a microring. The four input and output field describe propagation in all directions.

The system in Fig. 1 shows a microring coupled to a straight waveguide. Propagation is in both directions both in the bus and is in the ring. The sidewall roughness of the microring waveguide scatters the light travelling in the waveguide. The scattered light can either be transmitted along the waveguide in the same direction or back scattered in the opposite direction. To account for both propagation directions the system is described by a 4x4 scattering matrix:

$$\begin{bmatrix} b_1 \\ b_2 \\ b_3 \\ b_4 \end{bmatrix} = \begin{bmatrix} 0 & 0 & t & ik \\ 0 & 0 & ik & t \\ t & ik & 0 & 0 \\ ik & t & 0 & 0 \end{bmatrix} \begin{bmatrix} a_1 \\ a_2 \\ a_3 \\ a_4 \end{bmatrix} \quad (1)$$

Where a_i ($i=1,4$) are the four inputs and b_j ($j=1,4$) the four outputs. The real coefficients t and k account respectively for the field transmission and coupling of the bus to ring directional coupler with the additional condition $t_2 + k_2 = 1$.

The scattering matrix in Eq. (1) combines with the feedback of the ring as follows:

$$a_2 = ab_4 e^{-i\varphi} + \rho_c b_2 \quad (2.a)$$

$$a_4 = ab_2 e^{-i\varphi} + \rho_c b_4 \quad (2.b)$$

where $\rho_c = \rho e^{i\psi}$ is the reflection coefficient in the two directions arising from scattering due to roughness, a and φ are the field loss and phase accumulated over one round respectively.

Reflectivity ρ is a stochastic average and can be computed through the antenna theory as described in [12]. We approximate the phase of the reflection coefficient using the relation $\psi + \varphi = \pi/2$ that applies for lossless circuits [13]. Equations (4) and (5) in Ref [12]. present an integral and an analytic expression for ρ respectively. Reflectivity ρ can be viewed as a measure of the correlation length and the rms value of the surface roughness. a can be

expressed in terms of loss per unit length as $a = e^{-\alpha\pi R}$, where R is the ring radius and α is expressed in dB/cm .

The output at port Eq. (3) of the bus waveguide is obtained by solving Eq. (1) and Eq. (2) for $a_3 = 0$, and reads

$$T = \left. \frac{b_3}{a_1} \right|_{a_3=0} = \frac{\frac{t - ae^{-i\varphi}}{D} - t \frac{\rho_c^2}{D^2}}{1 - \rho_c^2 \left(\frac{t}{D} \right)^2} \quad (3)$$

whereas the reflection at port Eq. (1) reads

$$R = \left. \frac{b_1}{a_1} \right|_{a_3=0} = \frac{\rho_c}{D} \frac{t \frac{t - ae^{-i\varphi}}{D} - 1}{1 - \rho_c^2 \left(\frac{t}{D} \right)^2} \quad (4)$$

where $D = 1 - ate^{-i\varphi}$.

This model is a generalization of the approach described in Ref [14], which does not include backward propagation due to reflections.

3. Experiment and results

To test the theory we have fabricated a number of microrings with variable bus to ring gaps from $100nm$ to $590nm$ in steps of $10nm$. The bus waveguide, in the coupling region, is $220nm$ high and $400nm$ wide. The waveguide in the ring is $220nm$ high and $480nm$ wide. In order to make bending loss negligible compared to scattering loss the radii of the microrings were set to $10\mu m$. The test structure was designed as follows: each bus waveguide is coupled to five microrings placed in series far enough from each other not to interact. In each one of the five rings the radius is progressively increased by $25nm$, which corresponds to a difference in free spectral range of $1nm$ approximately. This is enough to make the five resonances perfectly distinguishable. Also, the amount of coupling of the bus to each of the microrings is varied by varying the gaps. By varying the gap by $100nm$ one can make sure to cover the whole spectrum from strongly over coupled to strongly under coupled. Additionally, the design presented above has been repeated 10 times and each time all the five gaps are increased by $10nm$. In this way we can map the microring response with gaps ranging from $100nm$ to $590nm$ with a $10nm$ variation. The spectral scans are obtained by employing an Agilent lightwave measurements system 8164B with integrated tunable laser source and photoreceiver. All scans have been taken with a spectral resolution of $60MHz$. Light is subsequently processed by a fiber polarization controller to ensure TE polarization and a lensed fiber to efficiently couple into the device under test.

Figure 2 presents a spectral scan taken in the middle of the L-band. The five resonances mentioned above are clearly visible and correspond to the following gaps from left to right: $110nm$, $210nm$, $310nm$, $410nm$ and $510nm$. The spectral scan shows clearly how the amount of coupling changes from high to low and the resonance quality factor degrades accordingly [15]. The three resonances on the left are over coupled while the two resonances on the right are under coupled. Furthermore, the under coupled cases show clear splitting in the resonances. This is due to roughness scattering and coupling into the backwards mode as described in the previous section. Noticeably, the over coupled cases do not present such resonances as a consequence of the fact that the broadening due to coupling from the bus into the ring is the strongest effect.

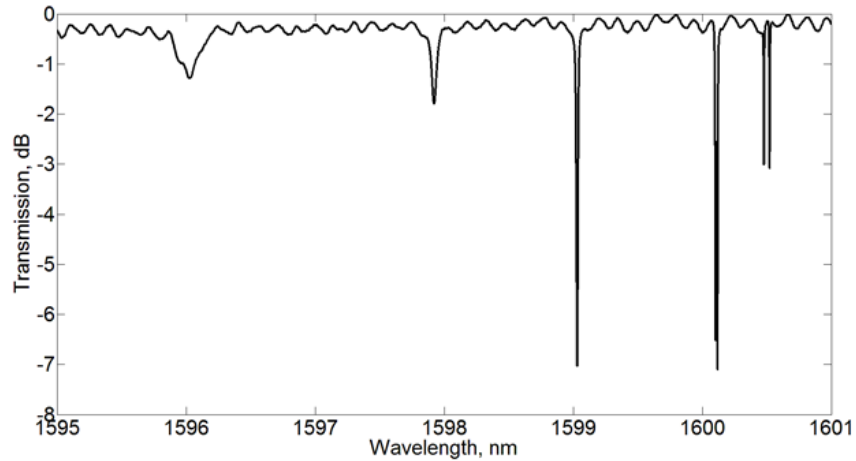


Fig. 2. Experimental measurement of five rings sharing a common bus waveguide. The bus to ring gaps were, left to right, 110nm , 210nm , 310nm , 410nm , 510nm . The radii were of the order of $10\mu\text{m}$ but slightly different to distinguish the individual spectra. The three spectra from left correspond to an over coupled condition, while the two spectra on the right correspond to an under coupled condition

Critical coupling occurs somewhere between 310nm and 410nm gaps. Interestingly, even by varying the gaps by 10nm from waveguide to waveguide, the critically coupled condition was never encountered. Due to this fact, methods that measure the waveguide loss by assuming the critical coupling condition is met are not very accurate since such condition is extremely intolerant and difficult to spot. In the over coupled condition the coupling prevails on other effects such as waveguide loss.

Vice versa in the under coupling condition, in which the microring quality factor is very large, the effect of the waveguide loss prevails on the bus to ring coupling. This is the ideal situation to accurately measure waveguide loss. However due to the resonance splitting one has to fit the experimental results with a model that includes such phenomenon, such as the one described above.

Figure 3 shows the intensity transmission $|T|^2$ for two values of the gap: 320nm in inset (a), and 390nm in inset (b). These two cases represent a slightly over and a slightly under coupled condition respectively. The transmission was computed following the approach described in the previous section for different values of the waveguide loss α , namely $1.3, 1.7$ and 2.1dB/cm .

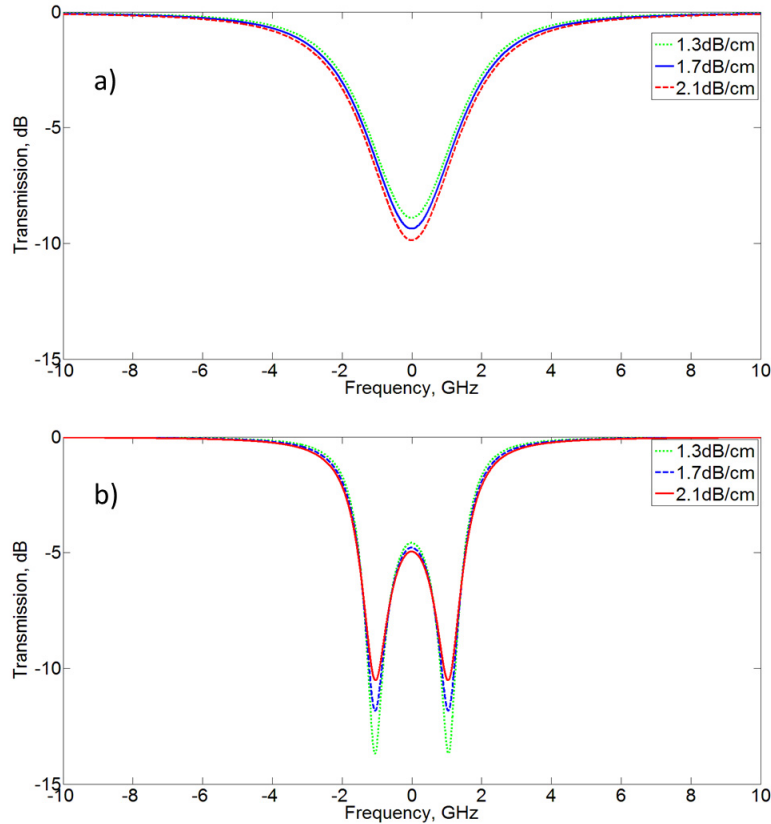


Fig. 3. Spectrum of intensity transmission from the bus for a microring with radius of $10\mu\text{m}$, gap 320nm (a), 390nm (b), and waveguide loss 1.3, 1.7, and $2.1\text{dB}/\text{cm}$.

The response in the under coupled regime is highly sensitive to α , which reflects on the depth of the split resonances. On the other hand in the over coupled regime losses do not affect the resonance as much. Furthermore the more one moves deep into the under (over) coupled regime the larger (lower) the sensitivity of the response as respect to α .

Figure 4 shows the impact of a variation in the absorption, α , caused by waveguide doping on the filter response. By varying the concentration of donor from $2 \times 10^{17}\text{cm}^{-3}$ to $3 \times 10^{17}\text{cm}^{-3}$ and $7 \times 10^{17}\text{cm}^{-3}$ one induces a loss of $\alpha = 2, 3$ and 5cm^{-1} respectively. It is clear that an increase in the loss due to absorption induces a change in the coupling condition by shifting it toward under coupling. Notice the position of the peaks is not altered meaning the amount of reflection stays constant. Therefore this method could be easily used to measure loss induced by doping, which is the case in active devices such as modulator and tunable filters.

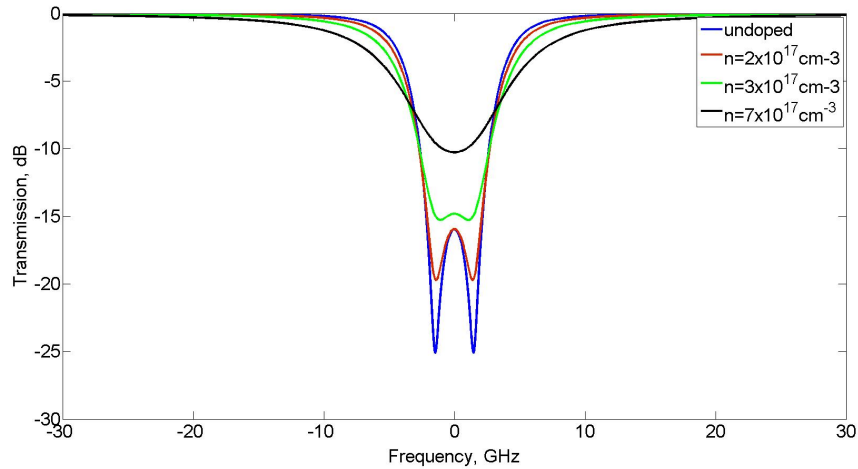


Fig. 4. Effect of absorption (α) caused by waveguide donor doping (n) on the transmission spectrum. Blue curve: undoped waveguide, red curve; $n = 2 \times 10^{17} \text{ cm}^{-3}$ ($\alpha = 2 \text{ cm}^{-1}$), green curve: $n = 3 \times 10^{17} \text{ cm}^{-3}$ ($\alpha = 3 \text{ cm}^{-1}$), black curve: $n = 7 \times 10^{17} \text{ cm}^{-3}$ ($\alpha = 5 \text{ cm}^{-1}$).

Figure 5 presents a comparison of some of the experimental spectral scans with the theoretical fit obtained from the model described above. The fitting is achieved by letting vary α , ρ and t . The ultimate goal of the fit is to estimate the propagation loss α . The three spectra depicted in insets (a), (b) and (c) respectively are such that back reflections ρ changes from 0.008 to 0.015 to 0.0303. In fact as the amount of light being back reflected increases the separation between the two peaks increases too, as already predicted in Ref [12].

The influence of the reflectivity coefficient on the amount of splitting may be understood from Eq. (2) in which each reflection introduces a phase shift of $\pi/2$. Assuming for instance an individual scattering center located in any position along the ring, the propagating light is in part transmitted and in part back scattered with a certain efficiency. The back-scattered light is phase shifted by $\pi/2$.

After a full round trip the same light is back reflected by the same scattering center in the forward direction thus adding another $\pi/2$ phase shift. After the back- and then the forward-scattering from each scattering center the phase is π shifted and a standing wave within the ring is formed. Being the standing wave and a travelling wave out of phase, their interaction leads to destructive interference. In fact when light is scattered inside a high Q cavity the resulting field may be high enough to cancel the field of the light propagating in the ring. For this reason the usual transmission dip that one would expect at resonance disappears, as shown in Fig. 4, and a black fringe appears growing larger when increasing the reflectivity ρ .

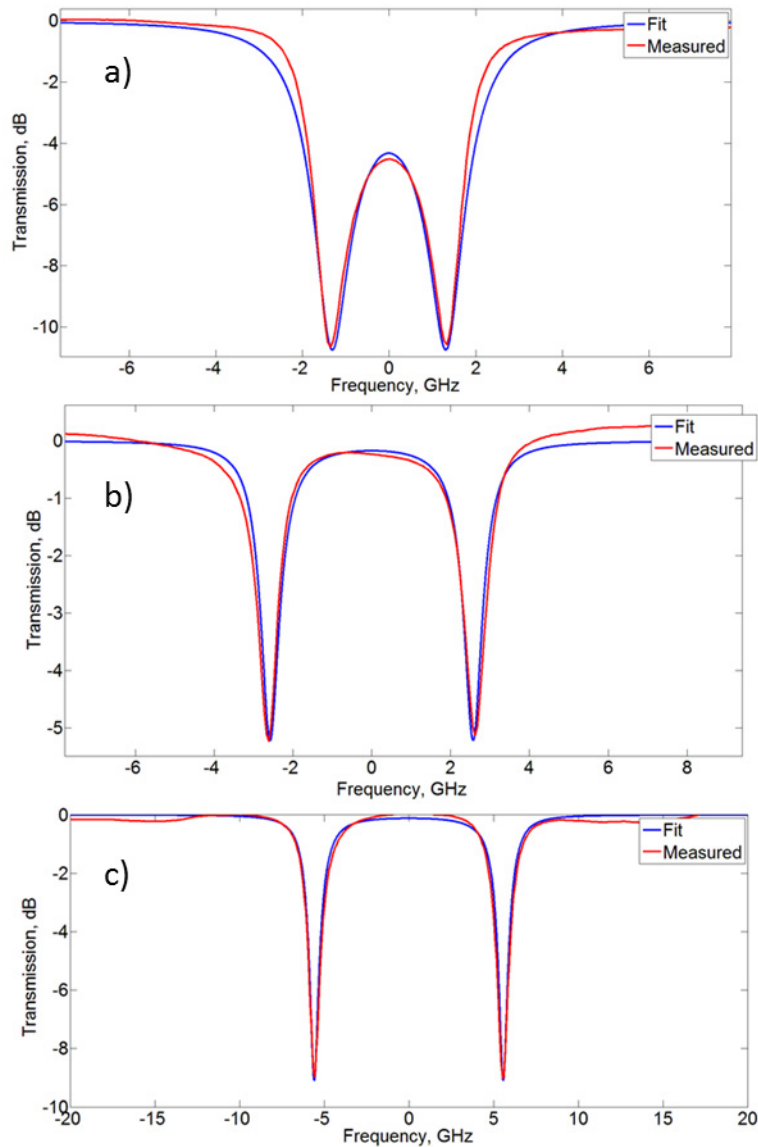


Fig. 5. Experimental (red line) and fit (blue line) are shown for three measurements. a) $\alpha = 2.3\text{dB/cm}$, $\rho = 0.008$, $t = 0.9965$ b) $\alpha = 1.7\text{dB/cm}$, $\rho = 0.015$, $t = 0.9991$ c) $\alpha = 2.1\text{dB/cm}$, $\rho = 0.0303$, $t = 0.9979$

On the contrary for $\rho = 0$ there would be only one transmission dip centered at the resonance. In other words the intracavity light scattering determines a standing wave similarly to what happens in a Fabry Perot cavity whereas the light propagating in the ring is a case of traveling wave cavity. The transmission dip cancellation is the result of the competition between the two types of cavity and the phenomenon and is more easily understood as a dark fringe in the middle of the transmission spectrum.

The amplitude of the reflection coefficient ρ depends on the correlation length of the correlation function describing the random edge roughness fluctuation [12]. Assuming a

constant value of average edge roughness, the reflectivity ρ increases with correlation length. In addition to back reflection due to surface roughness the radiation can even be reflected by the directional coupler which perturbs the propagation of the mode. However we verified with a 3D-FDTD simulation the magnitude of the coupler-induced reflection is orders of magnitude lower than value of ρ needed to fit the spectra. We conclude therefore the roughness only induces reflection. In fact, as confirmed by experiments, there is no correlation between the amount of coupling and reflectivity ρ .

Previous analyses, reported on in Ref [15], already envisaged the backscattering as possible cause of the resonance splitting in microring spectra. The authors presented a coupled mode theory describing the coupling between forward propagating mode in the microring and the backward mode induced by scattering from edge roughness. This model, equivalent to a double-ring second order filter, basically does not consider that each scattering point induces a first reflection in the backward direction that, and, being reflected a second time by the same center after a full round trip, becomes an out of phase forward reflection with respect to the radiation unaffected by scattering. In terms of physical model, the case in Ref [15], is a double ring second order filter whereas in the present model is the coupling between a ring and a Fabry-Perot like cavity. In Fig. 6 we report on, for the sake of comparison, an example of resonance splitting fitted with the two methods. The red curve is the experimental measurement, the blue curve corresponds to the method described in this paper and the quality of the fitting is excellent throughout the measured spectrum. The green curve, obtained with the previous approach, instead misses the tails and the discrepancy leads to a misleading evaluation of the waveguide loss.

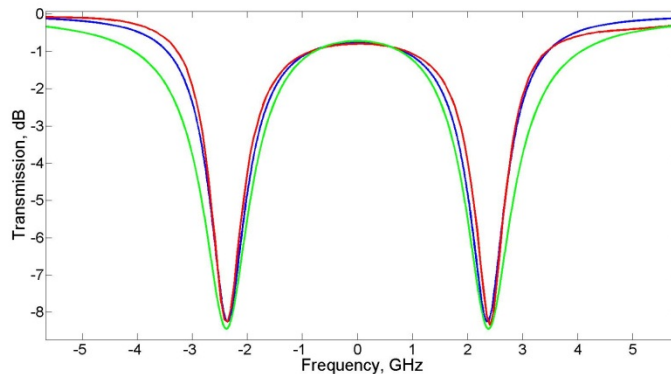


Fig. 6. Comparison of fitting models. Green curve: experimental, blue curve: present model fit, and green curve: double ring fit.

Finally Fig. 7 shows the statistics over 64 samples in terms of propagation loss thus obtained. The measured average loss is $1.7\text{dB}/\text{cm}$ and the standard deviation is $0.25\text{dB}/\text{cm}$. Notice the loss resulting from the erroneous fitting of the single resonances in Fig. 4 would have led to a value of $1.1\text{dB}/\text{cm}$.

The method described in the paper applies to ring waveguides fabricated with a good ring discretization in the mask. In the present case the discretization was 1 nm. Viceversa, for rough discretizations the measured value of waveguide loss would be affected by this extra effect.

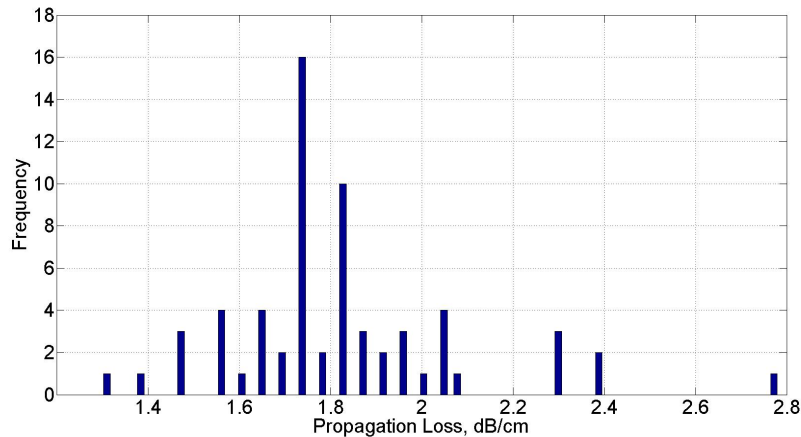


Fig. 7. Statistics of 64 samples gathered on waveguide loss. Average loss is $1.7\text{dB}/\text{cm}$, standard deviation $0.25\text{dB}/\text{cm}$.

4. Conclusions

In conclusion we presented a method for measuring the loss in submicron Si waveguides by means of fitting the transmission of a single under coupled microring structure. This method could also be useful as a test structure for inline characterization of the waveguide loss, assuming in this case vertically light coupling and extraction. In the discussion we have gone through the physical understanding of the double peaked observed transmission and we have concluded that it arises exclusively from intra cavity light scattering. We have shown also an example of measurement over a population of 64 rings giving an average loss of $1.7\text{dB}/\text{cm}$.

Acknowledgments

This work was supported by the Fully Laser Integrated Photonics (FLIP) program under APIC Corporation, supervised by Dr. Raj Dutt, and sponsored by the Naval Air Warfare Center - Aircraft Division (NAWC-AD) under OTA N00421-03-9-002. The authors thank Dr. Paola Galli for the helpful discussion on results.